

# Fractionation of a Diblock Copolymer in a Demixing-Solvent System

JIRÍ PODEŠVA,\* JAROSLAV STEJSKAL, and PAVEL KRATOCHVÍL

Institute of Macromolecular Chemistry, Czechoslovak Academy of Sciences, 162 06 Prague 6, Czechoslovakia

## SYNOPSIS

Phase behavior of a hydrogenated styrene/isoprene diblock copolymer in a dimethylformamide/methylcyclohexane demixing-solvent pair has been studied. At a fixed copolymer concentration (1% w/v), the scheme of phase behavior (temperature vs. mixed-solvent composition) of the system has been found to be complex, with several areas where various supramolecular structures are spontaneously formed. In a particular area of the scheme, a multistep demixing-solvent fractionation of the copolymer has been performed. The resulting fractions have been characterized and the data used to construct integral distribution functions of copolymer molar mass and copolymer composition. These functions have been compared with those obtained by a previously reported light-scattering characterization of the whole, unfractionated, nonhydrogenated precursor of the copolymer. © 1993 John Wiley & Sons, Inc.

## INTRODUCTION

We described in one of our previous papers<sup>1</sup> a special anionic synthesis of a styrene-isoprene diblock copolymer (coded as SI-w) with intentionally broadened molar-mass distributions of both blocks but without homopolymeric admixtures. Such a rather unusual modification of the synthesis yielded a product with so large a chemical heterogeneity that the corresponding parameters ( $P$  and  $Q$ , cf. Ref. 2) also were sufficiently high and could therefore be measured by static light scattering (SLS) with relatively good accuracy.<sup>1</sup>

In principle, the heterogeneity parameters of the compositionally "broad" copolymer SI-w can also be obtained by characterizing its fractions yielded by a preparative batchwise fractionation. We decided to apply a demixing-solvent fractionation (using, in our case, dimethylformamide [DMF]/methylcyclohexane [MCH] mixtures) that had been reported by Kuhn<sup>3-5</sup> to proceed predominantly according to chemical composition. This type of fractionation was

selected also with reference to our preceding results.<sup>6,7</sup>

Kuhn described, *inter alia*, a multistep demixing-solvent fractionation of chemically unmodified styrene-butadiene diblock copolymers,<sup>4</sup> but did not report any undesirable side reactions of the olefinic C=C bonds that would accompany the long-term exposure of the polymer to elevated temperatures of the fractionation and manifest themselves in cross-linking or degradation of the polymer. Nevertheless, to avoid completely such side reactions without massive stabilization of the fractionated copolymer solution, we decided to saturate specifically the olefinic double bonds of our polydiene blocks by hydrogenation by diimide.<sup>8-10</sup> It was demonstrated by some of us<sup>11</sup> that this polymer analogous reaction caused no detectable changes on the macromolecular level, such as microgel formation or chain scission, and, therefore, the distribution of molar mass and chemical composition of the substrate remained unaffected. Hence, the present results of the fractionation of the hydrogenated copolymer (coded as SI-w-h) may directly be compared with those of the characterization<sup>1</sup> obtained for its unfractionated and unsaturated precursor SI-w.

It was the aim of the present paper (i) to apply Kuhn's demixing-solvent fractionation procedure<sup>3-5</sup> to our copolymer SI-w-h, (ii) to interpret its results

\* To whom correspondence should be addressed.

in light of the conclusions<sup>6</sup> found for the demixing-solvent fractionations of statistical copolymers, and (iii) to compare the parameters of the molar-mass/composition distribution obtained by characterization<sup>1</sup> of the whole, unsaturated copolymer SI-w with those determined by characterization of the fractions of its saturated analog SI-w-h.

## NECESSARY TERMS AND RELATIONS

### Copolymers with Unspecified Microstructure

Generally, heterogeneity of a binary copolymer (monomeric units A and B) can be fully described by a two-dimensional distribution of molar mass  $M$  and chemical composition  $w$  (mass fraction of the component A), that is, by a function  $f_w(M, w)$  (see, e.g., Refs. 12 and 13). Approximations of this function were only exceptionally obtained from experiment<sup>14</sup> or calculated theoretically.<sup>15</sup> More frequently, one-dimensional, marginal differential mass distribution functions of  $M$  and  $w$ , viz.,  $f_w(M)$  and  $f_w(w)$  defined<sup>12</sup> as integrals of  $f_w(M, w)$  over all  $w$  or over all  $M$ , respectively, have been used. The distributions  $f_w(M)$  and  $f_w(w)$  can, in principle, be either estimated experimentally by a proper fractionation or approximated by a particular distribution function, e.g.,  $f_w(M)$  by the Schulz-Zimm (gamma) distribution:

$$f_w(M) = \frac{(h_c)^{y_c}}{\Gamma(y_c)} (M)^{y_c-1} \exp(-h_c M) \quad (1)$$

$$y_c = (a_c - 1)^{-1} \quad (2)$$

$$h_c = y_c / \bar{M}_{n,C} \quad (3)$$

where  $a_c$  is a ratio of mass-average molar mass of the copolymer ( $\bar{M}_{w,C}$ ) to number-average molar mass of the copolymer ( $\bar{M}_{n,C}$ ), and  $\Gamma$  is the gamma function. Examining the copolymer sample as a whole, the static light scattering (SLS) method is, in principle, able to yield two moments of the distribution  $f_w(M, w)$ , viz., parameters  $P$  and  $Q$ , as was demonstrated by Bushuk and Benoit.<sup>2</sup> Parameter  $P$  is a measure of interdependence between  $f_w(M)$  and  $f_w(w)$  and may assume both positive and negative values. Parameter  $Q$  characterizes the width of  $f_w(w)$  and is always positive.

In addition to  $P$  and  $Q$ ,  $\bar{M}_{w,C}$  can also be obtained by SLS from the solutions of a chemically heterogeneous copolymer,<sup>2</sup> whereas  $\bar{M}_{n,C}$  can be measured by, e.g., membrane osmometry (MO).

### Diblock Copolymers

For diblock copolymers, assuming random coupling of blocks (see, e.g., Ref. 16), relations have been derived<sup>12</sup> between the molar-mass distribution widths of the blocks, on the one hand, and the ratios  $P/\bar{M}_{w,C}$  and  $Q/\bar{M}_{w,C}$ , on the other; these relations hold regardless of the type of molar-mass distribution of the blocks and can be rewritten in a practical form<sup>1</sup>:

$$a_c = \bar{w}^2(a_A - 1) + (1 - \bar{w})^2(a_B - 1) + 1 \quad (4)$$

$$P/\bar{M}_{w,C} = [-\bar{w}^3(a_A + a_B - 2) + \bar{w}^2(a_A + 2a_B - 3) - \bar{w}(a_B - 1)]/D \quad (5)$$

$$Q/\bar{M}_{w,C} = (\bar{w}^4 - 2\bar{w}^3 + \bar{w}^2)(a_A + a_B - 2)/D \quad (6)$$

where  $D = \bar{w}^2(a_A + a_B - 2) - 2\bar{w}(a_B - 1) + a_B$ . The symbols  $a_A$  and  $a_B$  stand for the mass- to number-average molar mass ratios of the respective blocks, i.e., for  $\bar{M}_{w,A}/\bar{M}_{n,A}$  and  $\bar{M}_{w,B}/\bar{M}_{n,B}$ .

If experimental fractionation data solely are to be used without any assumption on the mathematical form of the functions  $f_w(M, w)$  or  $f_w(M)$  or  $f_w(w)$ , then a certain kind of cross-fractionation is necessary (see, e.g., Ref. 17). This approach is quite general and applicable also to other types of copolymers, but is very laborious, sometimes difficult to perform, and, as with any other type of fractionation, its efficiency is limited.

Throughout the following text, an *a priori* assumption of a particular type of distribution will be made. Under the assumption that the molar mass distributions of both blocks that form the diblock copolymer may be approximated by a Schulz-Zimm two-parameter distribution function, Stejskal and Kratochvíl<sup>18</sup> developed an analytical expression for  $f_w(w)$  with four parameters,  $\bar{w}$ ,  $z$ ,  $y_A$ , and  $y_B$ :

$$f_w(w) = \left[ \bar{w} \frac{\Gamma(y_A + y_B + 1)}{\Gamma(y_A + 1)\Gamma(y_B)} (z)^{y_A} \times (1 - z)^{y_B-1} + (1 - \bar{w}) \frac{\Gamma(y_A + y_B + 1)}{\Gamma(y_A)\Gamma(y_B + 1)} \times (z)^{y_A-1} (1 - z)^{y_B} \right] \frac{dz}{dw} \quad (7)$$

where

$$z = h_A w / [h_A w + h_B (1 - w)] \quad (8)$$

$$y_k = (a_k - 1)^{-1} \quad (k = A \text{ or } B) \quad (9)$$

$$h_k = y_k / \bar{M}_{n,k} \quad (k = A \text{ or } B) \quad (10)$$

The construction of, e.g., the marginal function  $f_w(w)$  according to eq. (7) requires the values of  $\bar{w}$ ,  $a_A$ ,  $a_B$ , and one of the three number-average molar masses ( $\bar{M}_{n,k}$ , where  $k = A, B$ , or  $C$ ). The parameters  $\bar{w}$  and  $\bar{M}_{n,k}$  can be obtained by, e.g., an appropriate analytical method (spectrometry or elemental analysis) and MO, respectively. In the "flowchart" in Figure 1, three ways of determining the remaining parameters,  $a_A$  and  $a_B$ , are given; two of them are based on the characterization of the whole, unfractionated diblock copolymer; one of them relies on the fractionation data:

- (i) The SLS method<sup>2,13</sup> yields  $\bar{M}_{w,C}$ ,  $Q$ , and  $P$  of the whole copolymer (middle column of Fig. 1). Using eqs. (4)–(6), the values of  $a_A$ ,  $a_B$ , and  $a_C$  may be calculated therefrom.
- (ii) A diblock copolymer is usually prepared by a consecutive anionic synthesis, i.e., after the first monomer (A) is consumed, the second monomer (B) is added to the living polyanions A. If the preparation is carried out so that a portion of living polyanions of type A is isolated before introducing monomer B into the mixture, it is possible to characterize the polymeric precursor, polyA, the molecular parameters of which are

identical to those of the block A in the copolymer. Then, for example, combining SLS and MO, we may obtain experimentally  $a_A$  and  $a_C$ . The missing value of  $a_B$ , as well as  $Q/\bar{M}_{w,C}$  and  $P/\bar{M}_{w,C}$ , may be calculated using eqs. (4)–(6) (right column of Fig. 1).

- (iii) If a simple fractionation of the copolymer is made, then the data obtained for all fractions in the form of a table (mass fraction  $W_i$ , chemical composition  $w_i$ , and molar mass  $M_i$ ,  $i = 1, 2, \dots, n$ ) can, in principle, be used for calculating  $\bar{w}$ ,  $\bar{M}_{w,C}$ , and  $\bar{M}_{n,C}$  according to

$$\bar{w} = \sum_i W_i w_i \quad (11)$$

$$\bar{M}_{w,C} = \sum_i W_i M_i \quad (12)$$

$$\bar{M}_{n,C} = \left[ \sum_i W_i / M_i \right]^{-1} \quad (13)$$

and for approximating  $P$  and  $Q$  by

$$P = \sum_i W_i (w_i - \bar{w}) M_i \quad (14)$$

$$Q = \sum_i W_i (w_i - \bar{w})^2 M_i \quad (15)$$

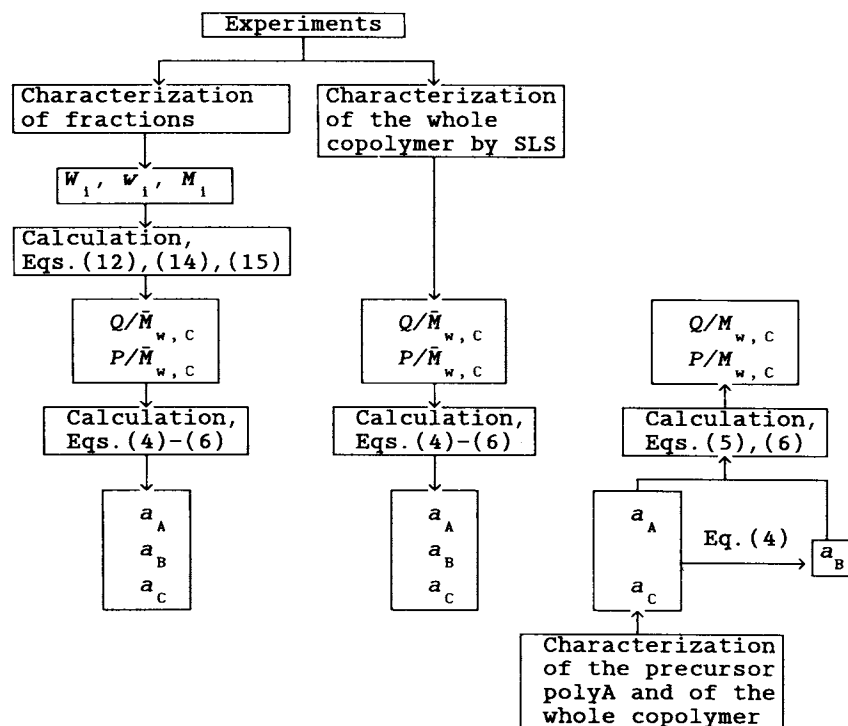


**Figure 1** A scheme of approaches to molecular characterization of chemically heterogeneous diblock copolymers: for explanation of the symbols, see text.

Obviously, the approximation of  $P$  and  $Q$  is in this case less adequate than in the case of a cross-fractionation.

Efficiency of any batchwise fractionation procedure depends on the number of fractionation steps but is generally low. For homopolymers, it leads to apparent molar-mass distributions that are often perceivably "narrower" than the true ones. In addition to this, an extra effect is operative with copolymers (including the diblock ones), namely, the interdependence of  $M$  and  $w$ . Two of the practically important consequences should be mentioned here: (a) All the copolymer fractions are both nonuniform in  $M$  and heterogeneous in  $w$  (therefore, the quantities  $w_i$  and  $M_i$  should for all fractions be replaced by  $\bar{w}_i$  and  $\bar{M}_{w,i}$ , respectively); and (b) the values of  $Q$ , obtained by calculation, are usually underestimated.

## EXPERIMENTAL

### Materials

Synthesis and a detailed characterization of the starting diblock copolymer of styrene (ST) and isoprene (IP), having relatively broad molar-mass distributions of both blocks and a code symbol SI-w, are described in Ref. 1. Hydrogenation of SI-w, yielding its saturated analog SI-w-h, is described in Ref. 11.

Dimethylformamide (DMF, Lachema, Czechoslovakia) was purified by a standard distillation procedure with benzene and water<sup>19</sup> to remove aminic impurities. After the benzene/water azeotropic mixture had been completely separated, CaH<sub>2</sub> was introduced into the remaining distilland to neutralize the traces of acidic admixtures; the suspension thus formed was distilled under reduced pressure to yield very pure DMF. Methylcyclohexane (MCH, Fluka) was distilled on a column.

Both DMF and MCH were checked by gas chromatography (GC) for purity (> 99.5% for MCH and a single peak for DMF were found). Auxiliary solvents like toluene and methanol (analytical grade, Lachema, Czechoslovakia) were used as received.

### Schemes of Phase Behavior

The coexistence curve of the polymer-free system DMF/MCH was obtained by analysis of conjugate phases. The starting mixture contained 40 wt % DMF and was homogeneous above ca. 53°C. At 10

different temperatures (30–51°C), the stock mixture, thermostated in a capped glass cylinder, was always equilibrated, and a small sample was taken from either conjugate phase by a syringe, equipped with a capillary. An equal volume amount of toluene was added to each sample directly in the syringe to make the mixture homogeneous even at room temperature. The composition of the resulting mixture was then determined by GC (see below).

A scheme of phase behavior of the system DMF/MCH/1 wt % SI-w-h (an approximation of the true phase diagram) was obtained by observing 14 solutions with gradually varying DMF/MCH ratios. The mass fraction of DMF,  $w_D$ , calculated with neglecting the presence of the copolymer, ranged from 0.125 to 0.650. Each solution was sealed in an ampule and submerged in a thermostat kept at 53°C. The temperature was then gradually decreased under frequent shaking of the ampules, and the appearance and behavior of the solutions (i.e., number of phases, color in side- and counterlight, viscosity, velocity of macroscopic phase separation, etc.) was observed.

### Fractionation

Since comparable volumes of the conjugate phases are often desirable with the demixing-solvent fractionation, a cylinder with a high length-to-diameter ratio has been used as a fractionation vessel. The contents of the vessel was stirred by a vertically sliding, magnetically operated, perforated PTFE disk.

The fractionation strategy was as follows:

- (i) The value of  $w_D$  of the starting solution was chosen so as to make the upper-to-lower phase volume ratio and therefore also the distribution of copolymer mass between both phases suitable (the copolymer fraction isolated from the upper phase had to be neither too big nor too little). This  $w_D$  was close to that corresponding to the maximum on the cloud-point curve (temperature vs.  $w_D$ ).
- (ii) The starting mixture was heated up to some 55°C in a thermostat and stirred to achieve a homogeneous solution. Then it was slowly cooled until the first signs of phase separation appeared. At this instant, the temperature decrease was stopped and the liquid phases were left to separate (usually overnight). The upper (MCH-rich) phase was always taken off the vessel and mixed with toluene to obtain a solution homogeneous even at room temperature. The copoly-

mer fraction was then isolated by usual (re)precipitation procedures.

- (iii) To control the upper-to-lower phase volume ratio and therefore also the distribution of copolymer mass between both phases in the next step, necessary amounts of DMF or MCH were added to the remaining lower phase before establishing the equilibrium. (As a consequence of this rather empirical procedure, the separation temperatures of consecutive fractionation steps did not show any trend.) Then, the new mixture was again heated and cooled as described in (ii), and the fractionation continued in the successive manner.

### Gas Chromatography

A Perkin-Elmer PE 8310 instrument, equipped with a flame-ionization detector, and a stainless-steel 3600 × 2 mm column, packed with 10% Carbowax 20 M on Chromosorb W 80/100 mesh, were applied. A temperature increase from 50 to 140°C in two steps was programmed. Under these conditions, the GC peaks of DMF, MCH, and toluene were well separated, and a calibration could be done.

### UV Spectroscopy

The method was used for determining the chemical composition of all fractions of SI-w-h. The absorption band, pertaining to the ST component, had its maximum at 260 nm. Respective neighboring minima, used for the calculation of the corrected absorbance value,  $A_c$ , lay at approximately 236 and 280 nm.

A calibration was done using several solutions of polystyrene in tetrahydrofuran (THF) and yielded the molar extinction coefficient  $\epsilon_{260} = 183.5 \pm 1.5 \text{ M}^{-1} \text{ cm}^{-1}$  ( $M = \text{mol L}^{-1}$ ). Values of  $A_c$  of an analyzed copolymer fraction, obtained also in THF, were plotted against a w/v concentration (in  $\text{g cm}^{-3}$ ) of the fraction; copolymer composition was calculated from the corresponding slope  $b$  (in  $\text{cm}^3 \text{ g}^{-1}$ ) using the relation

$$w_S = bM_S^0/(\epsilon_{260}10^3l) \quad (16)$$

in which  $M_S^0$  is the molar mass (in  $\text{g mol}^{-1}$ ) of the ST unit and  $l$  is the thickness of the UV cell (in cm). A Hewlett-Packard 8451-A diode array spectrometer with a 0.2 cm-thick cell was used at 25°C

for recording UV spectra in 230–300 nm wavelength range.

### Nuclear Magnetic Resonance

$^1\text{H}$ -NMR spectra were recorded partly with a PS-100 (JEOL) instrument (70°C, 100 MHz, and  $\text{CCl}_4$  as a solvent) and partly with an AC-300 Bruker spectrometer (60°C, 300.1 MHz, and  $\text{CDCl}_3$  as a solvent). In both cases, integrated peak intensities of aromatic and nonaromatic protons were used to calculate the  $w_S$ 's of those fractions of SI-w-h that were available in sufficient mass amounts (determination of  $w_S$  by UV needs some 10 mg of copolymer, whereas that by NMR, 40–50 mg).

### Static Light Scattering

SLS measurements were carried out at 25°C with a Sofica 42.000 instrument, equipped with a He — Ne laser (wavelength of the primary beam *in vacuo* was 633 nm, angular range 30–150°). THF was used as a solvent. Optical clarification of solutions was performed by ultracentrifugation directly in the scattering cells,<sup>20</sup> and the experimental data were treated by the Zimm method.<sup>21</sup> Refractive index increment values, necessary for the evaluation, were measured with a Brice-Phoenix Model BP-2000-V differential refractometer.

## RESULTS AND DISCUSSION

### Phase Behavior

MCH and DMF were chosen as a demixing-solvent pair because, at room temperature, the former component is a nonsolvent for polystyrene (the  $\theta$ -temperature<sup>22</sup> being 70.5°C) and a thermodynamically good solvent for hydrogenated polyisoprene ( $\theta < 0^\circ\text{C}$ ), whereas the opposite is true for the latter.

The scheme of the phase behavior of the system DMF/MCH/1% (w/v) SI-w-h is represented in Figure 2 (for the sake of completeness, also the phase diagram of a polymer-free DMF/MCH system is included). The practical applicability of the scheme is limited because (i) it was constructed from results of visual observations, (ii) it is valid only in a narrow interval of the copolymer concentration, in close vicinity of 1% (w/v), and (iii) overall chemical composition and molar mass—and thus also the phase behavior of the copolymer to be fractionated—undergo stepwise changes with successive collecting of

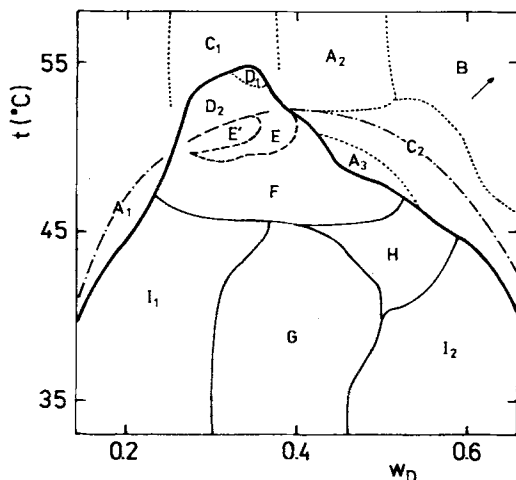


**Figure 2** A scheme of phase behavior (temperature  $t$  vs. mass fraction  $w_D$  of DMF) of the system DMF/MCH/1% ( $w/v$ ) of SI- $w$ - $h$ ; for explanation of the capital letters, see text; the thick solid line denotes the cloud-point curve in the presence of the copolymer; thin solid lines mark off individual areas of the diagram where more than one phase coexist; dash-and-dotted line corresponds to the coexistence curve in absence of the copolymer; dotted lines mean curves of association equilibria in the single-phase area; and dashed lines denote regions where various optical and hydrodynamic phenomena appear.

the fractions. Nevertheless, the scheme served as a useful tool for finding proper starting conditions and limitations to a preparative fractionation.<sup>†</sup>

The scheme is divided into two major regions by the thick solid line, above which the system is homogeneous (except for the area B) and below which a phase separation occurs. The most conspicuous feature of the scheme in Figure 2 is that each of the two major regions is subdivided into a large number of regions or areas having dramatically different properties.

In the areas denoted as  $A_1$ ,  $A_2$ , and  $A_3$ , the system is homogeneous but slightly opalescent and not colorless: It is yellowish when observed in the counterlight and intensively bluish when irradiated by the side light. It is very likely that supramolecular structures, such as the copolymer micelles,<sup>23</sup> are formed in these regions: We suggest that, at low

values of  $w_D$  ( $< ca. 0.26$ ,  $A_1$ ), blocks of hydrogenated polyisoprene constitute the shell, whereas the polystyrene blocks are concentrated in the core of the micelle; at higher  $w_D$  ( $0.35 < w_D < 0.5$ ,  $A_2$ ), reversed micelles (having a polystyrene shell) are probably present. Areas  $A_1$  and  $A_2$  are separated by a region  $C_1$  where the system is completely clear and colorless; it seems, therefore, that the system exists in  $C_1$  as a molecular solution.

The existence of the areas  $A_3$  (again, some supramolecular structures, probably micelles) and  $C_2$  (molecular solution) is rather unexpected. We can offer no unambiguous explanation of the fact that the system with  $w_D = 0.46$  passes, on cooling, from a micellar solution at  $t = 55^\circ\text{C}$  via a molecular solution at  $t = 51^\circ\text{C}$  to a micellar solution again, this time at  $t = 49^\circ\text{C}$ .

In the area B, SI- $w$ - $h$  is apparently separated from the solution by the precipitation ("sol-gel") mechanism without demixing the DMF/MCH solvent pair. In the direction of the arrow, the system becomes increasingly turbid (dispersionlike, "milky") without formation of layers or color effects. The boundaries between  $A_2$  and B and between B and  $C_2$  are rather fuzzy.

In the areas  $D_1$  and  $D_2$ , the system is separated into two colorless conjugate liquid phases, of which only one is completely transparent (the lower one in  $D_1$  and the upper one in  $D_2$ ), whereas the other shows a slight colorless "granulation" or a "raster" of unknown structure. SI- $w$ - $h$  is always present in both phases in isolable amounts so that a preparative multistep fractionation is feasible in  $D_1$  and  $D_2$ .

The area E and especially its subarea E' are the most interesting ones. Strong thixotropy is observed in E: When shaken, the system behaves as a mobile liquid, but when shaking is abruptly stopped, the mixture "freezes" to form a physical gel (able to trap air bubbles) that separates only very slowly into two liquid phases. However, the viscosity of the system is so high and, accordingly, diffusion of macromolecules between both phases is so slow, that establishing true phase equilibrium in finite time is unlikely. In addition to thixotropy, pronounced iridescence of the lower phase has been noticed in E': The phase scatters light very intensively and the lustrous scattered radiation displays various colors, depending on the angle of observation. Hypothetically, a lamellar structure of the mixture may be responsible for this phenomenon, but no attempt at a more detailed study has been done.

Here it should be stressed again that Figure 2 is not the true phase diagram where certain rules must be observed. The scheme represents a rather sim-

<sup>†</sup> To obtain a sufficient mass amount of each particular fraction during a preparative fractionation, and, at the same time, to avoid using enormous volumes of solvents, we had to apply a relatively high initial concentration of the copolymer (ca. 1 wt %) for both constructing the scheme and performing the fractionation. Also, some interesting association phenomena (see below), appearing at such high copolymer concentrations, might be inspiring for further study.

plified projection of several effects onto a plane and should be used as an orientation tool only.

Similar effects, i.e., thixotropy and iridescence, were also observed by us in the same demixing-solvent pair with Kraton G 1701 (Shell product), a commercially available material that is chemically identical to SI-w-h (ST/hydrogenated IP diblock copolymer). Direct comparison of the schemes of phase behavior of Kraton G 1701 and SI-w-h would be misleading, however, because the differences in the chemical composition ( $w_S \cong 0.34$  and  $0.50$ , respectively), in the chemical heterogeneity (Kraton is relatively homogeneous), and in the addition microstructure of the IP block are nonnegligible and cause rather different micellar behavior. (No Kraton having  $w_S \cong 0.50$  was available when our study was accomplished.) Though worth further attention, such effects were undesirable in our study because they hindered the fractionation.

Because of a very slow, or even blocked, phase separation, accompanied by strong turbidity of the whole system, the area  $F$  is also unsuitable for fractionation. The same is true for the area  $G$  where irreproducible behavior occurs and more than two phases are formed, and for the area  $H$  showing signs of copolymer precipitation. Boundary (or boundaries) between separated phases are always fuzzy in the areas  $F$ ,  $G$ , and  $H$ .

In contrast, rapid and distinct liquid-liquid demixing proceeds in the areas  $I_1$  and  $I_2$ , both separated phases being transparent. In the side light, the upper phase is bluish opalescent (micelle formation) and the lower one is colorless. However, fractionation is not feasible either in  $I_1$  or in  $I_2$  because all the copolymer is concentrated in the upper phase only and the lower one is always empty, as was proved by taking samples from the phases. Thus, with our system, fractionation is feasible in relatively small areas  $D_1$  and  $D_2$  only.

## Fractionation

Model calculations<sup>6</sup> showed that, assuming a copolymer with unspecified chain architecture and ignoring its possible supramolecular association, the difference between the solvent compositions of both conjugate phases (which decreases with increasing temperature of the phase separation) is of prime importance for the quality of fractionation:

At a temperature sufficiently lower than the critical one, where the difference in the demixing-solvent composition between both conjugate phases is large, the fractionation is expected to be governed much more by copolymer composition than by co-

polymer molar mass. Copolymer macromolecules having the content of one monomeric component (mass fraction  $w$ ) higher than a certain value (given largely by the solvent system) are concentrated almost exclusively in one of the conjugate phases, whereas the species with  $w$  lower than this value are present in the other phase. Thus, the heterogeneous copolymer sample with  $\bar{w}$  equal to or close to this value may very efficiently and "sharply" be divided into two fractions differing in their  $\bar{w}$ 's; they may differ also in their  $\bar{M}$ 's, but the extent of the difference is proportional only to the degree of interdependence between  $f_w(w)$  and  $f_w(M)$ : If these functions are independent ( $P = 0$ ), the difference in  $\bar{M}$  is nil. The two fractions thus obtained cannot usually be further fractionated in the same demixing-solvent system following, e.g., the triangular scheme. If  $\bar{w}$  of a heterogeneous sample is sufficiently higher or lower than the value discussed above, all the sample remains concentrated in one or another phase only.

On the other hand, when accomplished at temperatures closely below the maximum on the coexistence curve, a multistep fractionation is possible but the effect of  $M$  may become comparable with that of  $w$ .

These rules apply also to diblock copolymers, but, moreover, their complex phase behavior in demixing solvents and formation of supramolecular structures impose further limitations, as shown above. Thus, demixing-solvent fractionation seems to be even less favorable for diblock than for statistical copolymers. [Good fractionation results obtained for graft copolymers<sup>7</sup> can be explained by extremely broad  $f_w(w)$  of these materials and also by their small ability to form supramolecular structures, as compared to the block copolymers.]

These findings<sup>6</sup> seem to be less encouraging than the results reported by Kuhn.<sup>3-5</sup> Kuhn described,<sup>4</sup> *inter alia*, a routine straightforward successive fractionation of a styrene/butadiene diblock copolymer in the same demixing-solvent pair, i.e., DMF/MCH. In spite of the differences in the chemical nature of the nonaromatic blocks, the overall chemical compositions, and  $f_w(M, w)$  between SI-w-h and Kuhn's copolymer, one would intuitively expect similar limitations for the fractionation. In Kuhn's experiment,<sup>4</sup> however, eight fractions were isolated by a stepwise, decreasing-temperature fractionation run in a very broad temperature range (from 47 to 5.2°C) and no complicating effects were pointed out.

Phenomena such as thixotropy and iridescence were apparently not observed by Kuhn. The absence of these effects might, in principle, be explained by

**Table I Results of the Demixing–Solvent Fractionation of the Hydrogenated Diblock Copolymer of Styrene (ST) and Isoprene (IP) (SI-w-h) and Characterization of the Fractions**

Serial No. of Fraction	$W_i^a$	$I_{w,i}(M)^b$	$I_{w,i}(w)^b$	$w_{S,i}^c$	$10^{-3} \bar{M}_{w,i}^d$	$t^e$
1	0.121	0.371	0.941	0.660	323	51.5
2	0.175	0.914	0.560	0.560	427	52.0
3	0.061	0.652	0.678	0.580	372	51.3
4	0.028	0.198	0.866	0.635	260	50.4
5	0.190	0.526	0.279	0.445	330	50.8
6	0.184	0.092	0.092	0.210	174	49.0
7	0.098	0.261	0.423	0.490	297	50.0
8	0.144	0.754	0.780	0.620	404	50.0

<sup>a</sup> The mass fraction of the copolymer fraction  $i$  determined gravimetrically.

<sup>b</sup> The cumulative mass fraction of the copolymer fraction  $i$  calculated using eq. (19).

<sup>c</sup> The mass fraction of ST in the copolymer fraction  $i$  determined by UV and/or <sup>1</sup>H-NMR spectroscopy.

<sup>d</sup> Mass-average molar mass (in g mol<sup>-1</sup>) of the copolymer fraction  $i$  determined by SLS.

the fact that the initial concentration of the copolymer was, as a rule, several times lower than that in the present study, assuming the existence of a certain critical copolymer concentration, below which no association of macromolecules takes place.

Unlike in Ref. 4, in our fractionations, at temperatures lower by some 30–40°C than the critical one, the whole of the copolymer always concentrated in one phase. Also, for block copolymers with a broad distribution of chemical composition (e.g.,  $w$  between 0.12 and 0.50, cf. Fig. 4 in Ref. 4), a broad molar mass distribution (in any case broader than  $a_C < 1.02$ , as reported in Table 1 in Ref. 4) is common.<sup>12</sup>

It could be expected that, under the fractionation

conditions applied by us, two phenomena affect simultaneously the results of  $w_i$  and  $M_i$  of the fractions: (i) interdependence of  $f_w(M)$  and  $f_w(w)$ , and (ii) common unseparable influence of  $M$  and  $w$  upon the fractionation process. As no perceivable dependence of  $M_i$  or  $w_i$  on  $i$  can be noticed from the results of the fractionation (Table I), the phenomenon (ii) seems to be dominating (the difference between the lowest and highest values of  $M_i$  and  $w_i$  is substantially larger than the experimental error).

Fractionation data from Table I were used to calculate  $\bar{w}_S$ ,  $\bar{M}_{w,C}$ ,  $\bar{M}_{n,C}$ ,  $P$ ,  $Q$  [eqs. (11)–(15), respectively], and  $a_C = \bar{M}_{w,C}/\bar{M}_{n,C}$ . All values thus obtained are compared in Table II with those of unfractionated copolymer SI-w (cf. Ref. 1) measured

**Table II Comparison of Measured (by Static Light Scattering [SLS], Membrane Osmometry [MO], and Other Methods) and Calculated (from Fractionation Data) Values of Some Molecular Parameters**

	$\bar{w}_S$	$10^{-3} \bar{M}_{w,C}$	$10^{-3} \bar{M}_{n,C}$	$10^{-3} P$	$10^{-3} Q$	$a_C$
SI-w, measured	0.50 <sup>a</sup>	292 <sup>b</sup>	223 <sup>c</sup>	22 <sup>b</sup>	11.0 <sup>b</sup>	1.3 <sup>d</sup>
SI-w-h, calcd	0.491 <sup>e</sup>	326 <sup>f</sup>	296 <sup>g</sup>	10 <sup>h</sup>	5.9 <sup>i</sup>	1.1 <sup>d</sup>
SI-w-h, measured	0.50 <sup>j</sup>	320 <sup>j</sup>	—	—	—	1.3 <sup>j</sup>

<sup>a</sup> UV and/or H-NMR spectroscopy.

<sup>b</sup> SLS (Refs. 2 and 13).

<sup>c</sup> MO.

<sup>d</sup> Calculated as a ratio of the second and the third columns of this table.

<sup>e</sup> Eq. (11).

<sup>f</sup> Eq. (12).

<sup>g</sup> Eq. (13).

<sup>h</sup> Eq. (14).

<sup>i</sup> Eq. (15).

<sup>j</sup> From Ref. 11.



**Table III Comparison of Values of Some Molecular Parameters Obtained for SI-w and SI-w-h by Three Different Approaches According to Figure 1**

	SI-w-h Fractionation	SI-w	
		SLS <sup>a</sup>	SLS and MO <sup>b</sup>
$P/\bar{M}_{w,C}$	0.031	0.080	0.04
$Q/\bar{M}_{w,C}$	0.018	0.038	0.06
$a_A^c$	1.290	1.710	1.84
$a_B^c$	1.020	1.000	1.40
$a_C^c$	1.075	1.180	1.30

<sup>a</sup> SLS (Refs. 2 and 13).

<sup>b</sup> A combination of membrane osmometry and SLS.

<sup>c</sup> Mass- to number-average molar mass ratios calculated using Eq. (4)–(6).

by SLS and other methods (e.g., MO). Good agreement is seen for  $\bar{w}_S$  and  $\bar{M}_{w,C}$ . It is a natural consequence of the limited efficiency of the fractionation procedure that the values of  $Q$  and  $a_C$ , calculated from the fractionation data, are underestimated, and, accordingly, the value of  $\bar{M}_{n,C}$  is overestimated. In other words,  $f_w(M)$  and  $f_w(w)$  seem to be “narrower” when constructed from the fractionation data

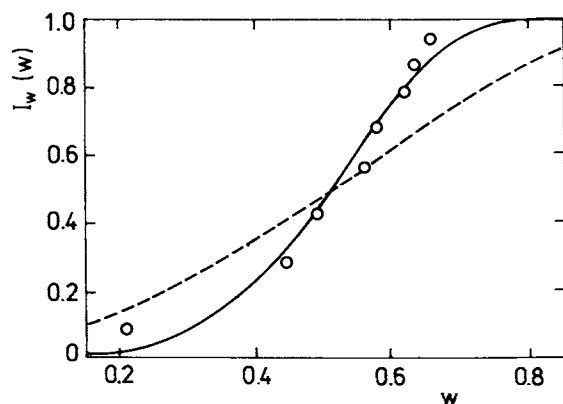


**Figure 3** Marginal integral mass distribution functions  $I_w(w)$  of chemical composition  $w$  (mass fraction of ST). Solid line: calculated from the fractionation data (experimental points) of the hydrogenated sample SI-w-h with  $a_A = 1.29$ ,  $a_B = 1.02$ ,  $\bar{M}_{n,A} = \bar{M}_{n,B} = 148 \times 10^3 \text{ g mol}^{-1}$  (left branch of the “flow chart” in Fig. 1); dashed line: calculated from the SLS and MO data of the nonhydrogenated precursor SI-w with  $a_A = 1.84$ ,  $a_B = 1.40$ ,  $\bar{M}_{n,A} = \bar{M}_{n,B} = 112 \times 10^3 \text{ g mol}^{-1}$  (right branch of the flow chart in Fig. 1); both lines were obtained by numerical integration of eq. (7).

in Table I (SI-w-h) than those obtained from the data in Ref. 1 (SI-w).

Another comparison, this time following the scheme in Figure 1, is accomplished in Table III. The second and the third columns of the table present data obtained for the whole, unfractionated SI-w (Ref. 1): The former gives experimental values of  $P/\bar{M}_{w,C}$  and  $Q/\bar{M}_{w,C}$  (SLS) from which  $a_A$ ,  $a_B$ , and  $a_C$  were calculated, whereas the latter contains measured values of  $a_A$  and  $a_C$  (SLS and MO) from which  $a_B$ ,  $P/\bar{M}_{w,C}$  and  $Q/\bar{M}_{w,C}$  were computed [in both cases, eqs. (4)–(6) were used]. Relatively good agreement between the values in the two columns (except for  $a_B$ , which is undoubtedly underestimated in the second column) gives evidence of internal consistency of the two experimental methods used. In contrast, all values, given in the first column and obtained from the data of the fractionation of SI-w-h, are perceptibly lower than those in the remaining columns (again with the exception of  $a_B$ ), the differences exceeding the experimental error. The explanation is the same as with Table II, namely, the low efficiency of the fractionation.

To make this comparison more lucid, we have plotted the marginal integral mass distribution functions  $I_w(w)$  and  $I_w(M)$ , defined by

$$I_w(w) = \int_0^w f_w(w) dw \quad (17)$$

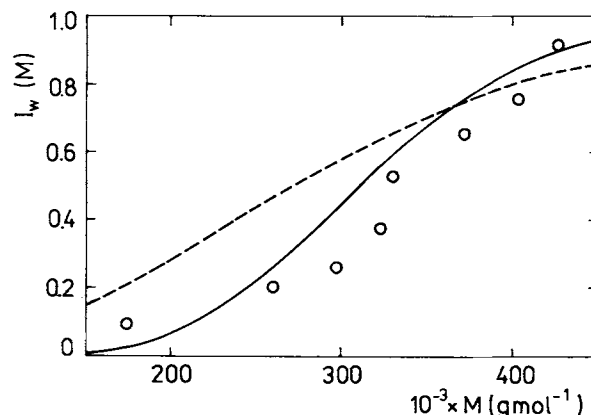


**Figure 4** Marginal integral mass distribution functions  $I_w(M)$  of molar mass  $M$ . Solid line: calculated from the fractionation data of the hydrogenated sample SI-w-h (experimental points) with  $a_C = 1.1$  and  $\bar{M}_{n,C} = 296 \times 10^3 \text{ g mol}^{-1}$ ; dashed line: calculated from the SLS and MO of the nonhydrogenated precursor SI-w with  $a_C = 1.3$  and  $\bar{M}_{n,C} = 223 \times 10^3 \text{ g mol}^{-1}$  (Table II); both lines were calculated by numerical integration of the Schulz-Zimm two-parameter distribution function [eq. (1)].

$$I_w(M) = \int_0^M f_w(M) dM \quad (18)$$

in Figures 3 and 4, respectively. To plot also the experimental points corresponding to the fractionation (Table I) into these figures, we approximated  $I_w(w)$  and  $I_w(M)$  by cumulative mass fractions  $I_{w,i}(w)$  and  $I_{w,i}(M)$  defined by a general formula:

$$I_{w,i} = (W_i/2) + \sum_{j=1}^{i-1} W_j \quad (19)$$

and rearranged the order of the fractions in Table I according to increasing  $M_i$  [ $I_{w,i} = I_{w,i}(M)$ ] and, alternatively, increasing  $w_i$  [ $I_{w,i} = I_{w,i}(w)$ ], respectively.

In both Figures 3 and 4, the S-shaped curve, calculated from the experimental points (fractions of SI-w-h, Table I) using eqs. (1)–(15) is distinctly steeper than that constructed from the data for the whole sample SI-w [eqs. (1)–(10)]; all four curves in Figures 3 and 4 were calculated under the assumption that  $f_w(M)$  of the whole copolymer (be it SI-w or SI-w-h) obeys the gamma distribution with the parameters  $a_C$  and  $M_{n,C}$ .<sup>‡</sup>

As the chemical reaction during which SI-w was converted into SI-w-h did not change the macromolecular structure (Ref. 11), it can be concluded that, as expected, the demixing–solvent fractionation proceeding near the top of the coexistence curve (where a combined effect of  $M$  and  $w$  is present) yields substantially narrower  $f_w(M)$  and  $f_w(w)$  than those of nonfractionation procedures.

## CONCLUSIONS

At a fixed copolymer concentration (1% w/v), the scheme of phase behavior (temperature vs. mixed-solvent composition) of the system of hydrogenated diblock copolymer of styrene and isoprene in dimethylformamide/methylcyclohexane mixtures is very complex: It contains several areas where various supramolecular structures (micelles, perhaps also lamellae) exist. Optical and other behavior of these

<sup>‡</sup> It was shown in Ref. 12 that, with the exception of a very broad chemical composition distribution, the choice of a type of the distribution function of the molar masses of the individual blocks was not crucial for an adequate description. Consequently, no alternative distribution function (such as the Wesslau or the Tung ones) needed to be checked in the present study.

structures makes the system an interesting subject of further study.

A multistep demixing–solvent fractionation of the copolymer is feasible only in a relatively small area closely below the maximum on the cloud-point curve. At lower temperatures, fractionation is hindered not only by supramolecular effects but also by the fact that the whole copolymer sample to be fractionated concentrates almost exclusively in one of the conjugate phases only.

A comparison of the distribution functions (i.e., marginal integral mass distribution functions of copolymer molar mass and copolymer composition) obtained from the data for the fractions with those gained previously by the light-scattering characterization of the whole, unfractionated, nonhydrogenated precursor shows that the former are distinctly narrower, as could be expected because of a limited efficiency of any fractionation technique.

## REFERENCES

1. J. Podešva, J. Stejskal, and P. Kratochvíl, *Macromolecules*, **20**, 2195 (1987).
2. W. Bushuk and H. Benoit, *Can. J. Chem.*, **36**, 1616 (1958).
3. R. Kuhn, *Makromol. Chem.*, **177**, 1525 (1976).
4. R. Kuhn, *Makromol. Chem.*, **181**, 725 (1980).
5. R. Kuhn, in *Polymer Alloys III*, D. Klemmner and K. C. Frisch, Eds., Plenum, New York, 1983, p. 45.
6. J. Podešva, J. Stejskal, O. Procházka, P. Špaček, and S. Enders, to appear.
7. J. Stejskal, D. Straková, P. Kratochvíl, S. D. Smith, and J. E. McGrath, *Macromolecules*, **22**, 861 (1989).
8. H. J. Harwood, D. B. Russel, J. J. A. Verthe, and J. Zymonas, *Makromol. Chem.*, **163**, 1 (1973).
9. L. A. Mango and R. W. Lenz, *Makromol. Chem.*, **163**, 13 (1973).
10. H. L. Hsieh and H. C. Yeh, *Polym. Prepr.*, **26**(2), 25 (1985).
11. J. Podešva, P. Špaček, and Č. Koňák, *J. Appl. Polym. Sci.*, **44**, 527 (1992).
12. J. Stejskal and P. Kratochvíl, *Polym. J.*, **14**, 603 (1982).
13. P. Kratochvíl, *Classical Light Scattering from Polymer Solutions*, A. D. Jenkins, Ed., Elsevier, Amsterdam, 1987.
14. G. Glöckner, J. Stejskal, and P. Kratochvíl, *Makromol. Chem.*, **190**, 427 (1989).
15. O. Procházka and P. Kratochvíl, *J. Polym. Sci. Polym. Phys. Ed.*, **22**, 501 (1984).
16. T. Kotaka, N. Donkai, and T. I. Min, *Bull. Inst. Chem. Res. Kyoto Univ.*, **52**, 332 (1974).
17. J. Stejskal, P. Kratochvíl, and D. Straková, *Macromolecules*, **14**, 150 (1981).

18. J. Stejskal and P. Kratochvíl, *Makromol. Chem.*, **188**, 2435 (1987).
19. W. Bunge, in *Methoden der Organischen Chemie, Band I/2*, J. Houben and T. Weyl, Eds., Georg Thieme Verlag, Stuttgart 1959, p. 765.
20. L. Mrkvičková-Vaculová and P. Kratochvíl, *Coll. Czech. Chem. Commun.*, **37**, 2015 (1972).
21. B. H. Zimm, *J. Chem. Phys.*, **16**, 1099 (1948).
22. J. Brandrup and E. H. Immergut, Eds., *Polymer Handbook*, Wiley-Interscience, New York, 1966, p. IV-171.
23. Z. Tuzar and P. Kratochvíl, *Surface and Colloid Science*, E. Matijevic, Ed., Vol. 15, Plenum Press, New York, 1993, p. 1.

Received July 23, 1992

Accepted November 30, 1992